Kinetics of Reactions of H Atoms With Ethane and Chlorinated Ethanes

Mikhail G. Bryukov,† Irene R. Slagle, and Vadim D. Knyazev*

Department of Chemistry, The Catholic University of America, Washington, D.C. 20064

Received: February 18, 2001; In Final Form: April 27, 2001

The reactions of H atoms with ethane and three chlorinated ethanes (C_2H_5Cl, 1,2-$C_2H_4Cl_2$, and CH_3CCl_3) have been studied experimentally using the Discharge Flow/Resonance Fluorescence technique over wide ranges of temperatures. The rate constants were obtained in direct experiments as functions of temperature. Literature data on the reactions of H atoms with ethane and chloroethane are analyzed and compared with the results of the current investigation. A transition-state-theory model of the reaction of H atoms with ethane was created on the basis of ab initio calculations and analysis of the experimental data and was used to extrapolate the latter to temperatures outside of the experimental ranges.

I. Introduction

Widespread use of incineration as a treatment of hazardous industrial wastes, including chlorinated hydrocarbons (CHCs), has stimulated the development of research directed at mechanistic and kinetic modeling of chlorinated hydrocarbon combustion. Fundamental knowledge of mechanisms, specific pathways, and rate constants of important elementary reactions is of key importance to the success of such modeling. Among the most important and sensitive reactions involved in the currently used mechanisms of combustion of chlorinated hydrocarbons are the reactions of Cl and H atoms with the main compounds that are being burned.[1−9] In CHC/O_2 and CHC/hydrocarbon/O_2 flames, reactions of Cl and H atoms with CHCs together with unimolecular decomposition are the major channels of consumption of CHCs.[1−5,7−14] The results of numerical simulations demonstrate that the rates of CHC destruction and concentrations of active species are highly sensitive to the rates of Cl + CHC and H + CHC reactions.

In a recent article,[15] we reported our experimental and computational study of the reactions of H atoms with methane and four chlorinated methanes. Here, we present the results of our experimental investigation of the reactions of H atoms with ethane and three chlorinated ethanes conducted over wide ranges of temperatures

$$H + C_2H_6 \rightarrow H_2 + C_2H_5 \qquad (467-826\ K) \qquad (1)$$

$$H + C_2H_5Cl \rightarrow \text{products} \qquad (483-826\ K) \qquad (2)$$

$$H + 1,2\text{-}C_2H_4Cl_2 \rightarrow \text{products} \qquad (483-826\ K) \qquad (3)$$

$$H + CH_3CCl_3 \rightarrow \text{products} \qquad (358-850\ K) \qquad (4)$$

Numbers in parentheses indicate the experimental temperature ranges of the current work.

Of all reactions of H atoms with chlorinated ethanes, only reaction 2 has been studied previously. Triebert et al.[16] used a discharge flow reactor coupled to a quadrupole mass spectrometer to obtain the rate constant of reaction 2 at room temperature and a pressure of 3 Torr. In contrast, the kinetics of reaction 1, that of H atoms with ethane, has been studied experimentally by numerous groups over the past four decades. Reviews of literature can be found in refs 17−19. However, only in four studies[20−23] was the rate of reaction 1 measured by direct experimental methods. Furthermore, only in the work of Jones, Morgan, and Purnell[22] was reaction 1 sufficiently isolated from complicating side reactions, so that no stoichiometric corrections to the measured reaction rate had to be applied.

The experimental technique used in the current work, discharge flow reactor with resonance fluorescence detection of H atoms, has an excellent sensitivity to hydrogen atoms (detection limit of $<10^8$ atoms cm^{-3}). This sensitivity enables experiments with very low initial H concentrations ($\leq 10^{11}$ atoms cm^{-3}), thus ensuring the absence of any complications due to potential fast secondary reactions.

The current article is organized as follows. Section I (current) is an introduction. The experimental method, procedures, and results are reported in section II. In section III, a transition state theory model of reaction 1 is presented. The results are discussed in section IV.

II. Experimental Section

Rate constant measurements were conducted in a heatable tubular flow reactor under pseudo-first-order conditions with a large excess of molecular substrate. H atoms were detected by resonance fluorescence and their decay measured as a function of contact time over a wide range of experimental conditions.

II.1. Experimental Apparatus. Details of the experimental apparatus have been described previously,[15] and thus, only a brief description is given here. H atoms were generated in the sidearm of a heated tubular quartz or Pyrex reactor by a 2.45 GHz microwave discharge in a H_2/He mixture. Hydrogen atoms formed in the discharge area were carried through the reactor by a flow of helium and their concentration was monitored by resonance fluorescence in the detection zone located downstream. The molecular substrate ($C_2H_xCl_y$) was introduced through a quartz movable injector.

* To whom correspondence should be addressed. E-mail: knyazev@cua.edu.

† Because of different methods of transliteration from the Cyrillic alphabet, this name has also been spelled as *Mikhail G. Brioukov.*

10.1021/jp0106505 CCC: $20.00
Published on Web 06/20/2001

Pressure in the reactor was monitored through outlets positioned at the ends of the heated zone. The viscous pressure drop in the heated zone of the reactor was obtained by measuring the difference in pressure values obtained upstream and downstream of the heated zone and by subsequent interpolation. The range of typical values of the viscous pressure drop in the working part of the heated zone was 0.03−0.15 Torr. The uniformity of the temperature profiles in this region (20−30 cm in length) was at least 5 K (maximum temperature differences were 5 K at the highest temperature used and less at lower temperatures).

Various aspects of the discharge flow technique of measuring rate constants of gas phase chemical reactions have been extensively discussed in the literature.[24−27] These discussions are not repeated here. Care was taken to ensure that, under all experimental conditions used in the current work, the plug-flow approximation was valid. The only exception to the plug flow approximation was the minor, although nonnegligible, contribution of axial diffusion of H atoms. Corrections for axial and radial diffusion were introduced into the experimentally obtained atom decay rates (vide infra).

Two reactors were used in these experiments: a quartz reactor with an internal diameter (i.d.) of 1.93 cm and a Pyrex reactor with i.d. = 4.66 cm. The reactor surface, the surface of the movable injector, and the inside of the discharge tube were treated to reduce heterogeneous loss of H atoms first by soaking in a 5% aqueous solution of ammonium bifluoride for 30 min and then by the method of Sepehrad et al.[28] The resultant values of the first-order wall loss rate constant, k_w, were always below or equal to 20 s^{-1}. Typical values of k_w were ≈4 s^{-1} for the Pyrex reactor and 12−20 s^{-1} for the quartz reactor. Reactors of different diameters were used to rule out potential contributions of heterogeneous reactions to the rate constant values obtained in the experiments (vide infra).

H atom resonance fluorescence (Lyman-α, 121.6 nm) was induced by light from a discharge flow resonance lamp[29,30] and detected by a solar blind photomultiplier (EMR model 542-G-09). A molecular oxygen optical filter (140 Torr of O_2, optical path length 3 cm)[31] effectively cut off radiation at all wavelengths in the range corresponding to the peak of the photomultiplier sensitivity (115−170 nm) except for the four narrow gaps in the spectrum of O_2 (between 115 and 122 nm), one of which coincides with the Lyman-α hydrogen atom line (121.6 nm).[30]

The sensitivity of the atom detection system to H atoms was determined by titration with NO_2 (rate constant of the $H + NO_2$ reaction is 1.4×10^{-10} cm^3 $molecule^{-1}$ s^{-1}).[32] Typical concentrations at which the fluorescence signal was equal to the scattered light from the discharge flow lamp were ≈10^9 atom cm^{-3}. The sensitivity limit (defined by unity signal-to-noise ratio) was $<10^8$ atom cm^{-3}. In the titration experiments, relatively high concentrations of H atoms had to be used (≈10^{12} atoms cm^{-3}). Such concentrations caused some degree of self-absorption of light at the Lyman-α line, resulting in a nonlinear dependence (saturation) of the resonance fluorescence signal on the atom concentration. Thus, the calibration of the H atom signal based on measuring the decrease in fluorescence signal upon addition of a small flow of NO_2 to the reactor yielded underestimated values of sensitivity coefficients (defined as the ratio of signal to H concentration). Therefore, the values of the initial concentrations of H atoms used in the experiments to determine the rate constants of reactions 1−4 (listed in Table 1) are somewhat overestimated and should be understood as upper limits to $[H]_0$.

Molecular substrates ($C_2H_xCl_y$) were stored undiluted in Pyrex reservoirs. Flows of these reagents into the reactor were determined by measuring the pressure drop in a calibrated volume over time. That the measured flows were independent of the surface-to-volume ratio of the calibrated volume was verified to ensure the absence of interference from heterogeneous absorption and desorption processes on the walls of vacuum manifold. Flows of molecular hydrogen to the atom-producing discharge were measured in a similar way. It was found that the typical dissociation efficiency of the discharge was ≈20%. This resulted in the concentrations of undissociated H_2 in the reactor being approximately a factor of 2 to 3 higher than the initial H atom concentrations.

II.2. Reaction Rate Measurements. All experiments to measure the rate constants of reactions 1−4 were conducted under conditions of a large excess of molecular substrate ($195 \leq [C_2H_xCl_y]/[H]_0 \leq 1.6 \times 10^5$). Initial concentrations of H atoms in the detection zone were in the range $(2.2 - 8.4) \times 10^{10}$ atoms cm^{-3}. (These values of $[H]_0$ should be understood as upper limits to the actual concentrations of hydrogen atoms because the calibration procedure underestimated the calibration coefficient values, as described in subsection II.1.) Exact knowledge of the H atom concentrations is not needed for the determination of rate constants because all experiments were conducted under pseudo-first-order conditions. The rate of heterogeneous loss of H atoms on the walls of the reactor and the movable injector were regularly measured (in the absence of molecular substrate). In these measurements, the time of contact between the H atoms generated in the discharge and the walls was varied by changing the flow velocity (by means of switching the flow of helium carrier gas between a fixed inlet located near the H atom source and the movable injector at various positions of the latter) with no alterations of the conditions in the discharge and monitoring the resultant changes in the signal of H atoms in the detection zone. The H atom wall loss rate constants were in the range 4−20 s^{-1}.

The time of contact between the molecular substrate and H atoms was varied by changing the position of the movable injector. Under the experimental conditions used, plug flow conditions are satisfied (except for a required correction for axial diffusion, vide infra) and increments of contact time can be obtained by dividing the corresponding changes in the length of the contact zone by the bulk flow velocity, V. The tip of the movable injector was always kept within the heated working zone of the reactor.

The total signal (counts s^{-1}) detected by the photomultiplier consisted of three components: fluorescence of H atoms (S_H), the photomultiplier dark current (less than 1 count s^{-1}), and the scattered light originating from the resonance lamp and reflected by the walls of the detection system (typically, ≈30 counts s^{-1}). The contributions from the dark current and the scattered light were measured directly in the absence of H atoms but with the molecular substrate present (to account for possible absorption of the scattered light) and later subtracted from the total signal to obtain S_H.

The effective first-order rate constant values, k'_{OBS}, were obtained from least-squares-fits of the H atom fluorescence signal S_H to the equation

$$\ln(S_H) = \text{constant} - k'_{OBS}\, x\, V^{-1} \qquad \text{(I)}$$

where x is the distance between the tip of the movable injector and the detection zone and V is the bulk flow velocity in the reactor. Examples of experimentally obtained $\ln(S_H)$ vs x dependences are presented in Figure 1. The observed values of

TABLE 1: Conditions and Results of the Experiments to Measure Rate Constants of the Reactions of H Atoms with Ethane and Chlorinated Ethanes

no.[a]	T/K	P/Torr[b]	$[C_xH_yCl_z]$ range/ 10^{12} molecule cm^{-3}	k_0/s^{-1} [c]	V/cm s^{-1} [d]	$[H]_0/10^{10}$ molecule cm^{-3}	$(k'_{OBS}D/V^2)_{max}$	$k_i/10^{-14}$ cm^3 molecule^{-1} s^{-1} [e]
				H + C_2H_6 → H + C_2H_5				
1−1	467	8.01−8.03	1050−4340	−0.9 ± 2.5	861−891	3.4	0.026	1.04 ± 0.10
1−2*	491	2.66−2.86	996−4390	2.0 ± 4.6	738−763	2.7	0.127	1.42 ± 0.16
1−3*	534	1.90−2.01	109−2790	2.3 ± 4.6	740−769	6.8	0.241	2.86 ± 0.29
1−4*	586	3.85−3.98	274−2520	5.4 ± 5.6	931−949	8.4	0.185	5.45 ± 0.43
1−5	612	6.07−6.15	426−2070	−3.4 ± 8.2	2113−2180	6.9	0.037	7.88 ± 0.59
1−6*	637	3.69−3.76	74.5−1340	2.4 ± 2.8	1001−1021	4.6	0.195	10.8 ± 0.4
1−7	693	2.03−2.06	99.2−1110	10 ± 13	1788−1858	6.6	0.215	22.1 ± 2.0
1−8	705	5.84−6.03	86.9−934	11 ± 14	1746−1803	5.9	0.065	17.5 ± 2.3
1−9*	748	1.92−1.93	74.1−249	1.5 ± 3.1	1037−1060	2.3	0.203	25.9 ± 1.9
1−10	776	1.97−2.02	88.7−484	7.6 ± 15	1826−1878	3.6	0.226	44.0 ± 5.0
1−11	796	2.08−2.13	78.9−394	0.6 ± 11	2075−2173	3.0	0.145	44.5 ± 4.1
1−12	826	2.04−2.07	56.6−386	11 ± 15	2269−2296	7.2	0.160	53.6 ± 7.2
1−13	826	1.96−2.00	56.3−787	10 ± 16	2870−3008	6.0	0.185	49.7 ± 3.5
				H + C_2H_5Cl → products				
2−1*	483	3.94−4.09	549−1980	−0.5 ± 1.6	763−775	6.7	0.079	2.64 ± 0.12
2−2	512	8.00−8.10	422−1580	1.4 ± 4.4	512−518	2.5	0.021	3.72 ± 0.40
2−3*	534	3.94−4.03	502−1410	−0.2 ± 3.6	845−858	2.5	0.103	4.98 ± 0.39
2−4*	586	3.48−3.53	265−1150	2.5 ± 4.0	901−916	3.9	0.171	9.07 ± 0.68
2−5*	637	4.01−4.07	77.3−708	0.6 ± 4.1	1017−1042	4.5	0.157	17.2 ± 1.0
2−6*	687	3.92−3.97	133−619	2.8 ± 9.0	1082−1097	7.7	0.207	26.2 ± 2.5
2−7	713	6.05−6.07	164−526	7 ± 14	1683−1700	2.2	0.077	35.1 ± 4.4
2−8*	748	3.90−3.96	21.9−382	4.3 ± 4.5	1180−1195	7.1	0.186	38.3 ± 2.1
2−9	796	2.05−2.08	59−260	5.2 ± 6.8	2429−2484	3.0	0.121	70.5 ± 4.2
2−10	826	1.92−1.94	43.1−228	5.7 ± 4.8	3156−3181	6.9	0.100	95.5 ± 3.9
2−11	826	1.96−1.98	77.6−337	4 ± 23	2273−2325	6.7	0.232	88.4 ± 10.3
				H + 1,2-$C_2H_4Cl_2$ → products				
3−1*	483	3.86−4.05	540−1640	0.4 ± 2.5	628−766	3.9	0.082	2.05 ± 0.21
3−2	511	8.01−8.05	299−1210	1.7 ± 2.3	884−901	2.5	0.030	3.76 ± 0.30
3−3*	534	1.83−1.91	347−1550	1.1 ± 3.1	700−740	5.0	0.242	3.96 ± 0.30
3−4*	586	3.82−4.07	311−1160	−1.0 ± 3.3	917−927	4.1	0.158	9.72 ± 0.52
3−5*	637	3.87−3.92	207−744	3.1 ± 4.4	1004−1013	7.9	0.170	16.32 ± 0.91
3−6*	687	3.87−3.96	126−616	1.0 ± 8.8	1073−1095	6.8	0.231	27.7 ± 2.4
3−7*	748	3.83−3.87	54.6−371	−4.6 ± 5.1	1171−1187	6.4	0.231	49.4 ± 2.3
3−8	796	1.95−1.98	91.6−371	−4 ± 10	2178−2236	2.3	0.206	71.2 ± 4.6
3−9	826	1.96−1.98	51.2−302	0 ± 10	2131−2187	7.3	0.210	78.5 ± 6.1
3−10	826	1.95−1.99	50.2−310	−8 ± 17	2944−3005	6.6	0.126	77.7 ± 8.6
				H + CH_3CCl_3 → products				
4−1	358	7.93−8.03	548−2950 [f]	1.7 ± 2.2	663−670	3.1	0.126	1.21 ± 0.13
4−2	371	5.86−6.00	457−3710	2.2 ± 4.0	708−733	4.7	0.211	1.56 ± 0.20
4−3	384	3.00−3.05	190−2790 [f]	1.9 ± 2.5	1252−1272	5.2	0.128	1.65 ± 0.13
4−4*	399	3.95−4.03	533−2020	−0.6 ± 2.4	632−641	7.9	0.088	2.96 ± 0.18
4−5*	437	3.64−3.74	534−2060	3.0 ± 3.2	678−696	6.1	0.126	4.28 ± 0.24
4−6*	437	3.64−3.72	292−1420	3.5 ± 4.2	840−859	6.6	0.087	5.04 ± 0.53
4−7	452	5.97−6.02	133−1320	6.1 ± 4.7	856−874	3.4	0.138	6.45 ± 0.65
4−8*	483	4.04−4.12	397−1350	−3.5 ± 6.5	756−764	5.1	0.118	9.85 ± 0.75
4−9	510	3.03−3.05	66.4−721	−1.7 ± 3.7	1842−1886	6.6	0.126	18.75 ± 0.96
4−10*	534	4.07−4.10	85.8−564	0.0 ± 6.1	846−861	6.1	0.211	17.8 ± 1.8
4−11*	586	3.64−4.02	106−435	−4.8 ± 5.0	912−950	6.0	0.128	32.6 ± 1.8
4−12*	637	3.82−3.87	80.7−306	−2.3 ± 9.0	994−1021	6.2	0.088	53.6 ± 5.0
4−13	682	2.96−2.99	32.4−205 [f]	3.2 ± 6.2	1894−1946	2.2	0.126	106.1 ± 5.5
4−14	727	4.05−4.10	15.3−192	13 ± 10	1518−1567	3.2	0.087	162 ± 11
4−15*	748	4.23−4.26	15.7−122	−0.6 ± 9.0	1182−1205	4.5	0.138	141 ± 11
4−16	778	5.98−6.09	15.3−96.4	4.5 ± 9.9	1830−1867	6.5	0.118	212 ± 18
4−17	805	3.98−4.28	17.3−191	23 ± 32	3422−3487	3.4	0.126	223 ± 32
4−18	826	1.95−1.96	16.4−64.4 [f]	4 ± 12	2051−2094	2.6	0.211	290 ± 30
4−19	850	2.91−2.96	9.35−87.7	11 ± 11	2068−2188	4.8	0.128	329 ± 23
4−20	850	2.90−2.92	19.1−83.4	9 ± 12	2795−2827	6.4	0.088	334 ± 25

[a] Experiment number. A Pyrex reactor with internal diameter (i.d.) 4.66 cm was used in experiments marked with * and a quartz reactor with i.d. = 1.93 cm was used in unmarked experiments. [b] Minor variations in pressure are due to changes in flow conditions upon addition of large flows of molecular substrate ($C_2H_xCl_y$). [c] Zero-abscissa intercept on the k' vs $[C_2H_xCl_y]$ dependence (see discussion of formula IV in the text). [d] Bulk flow velocity range. Minor variations in flow velocity are due to changes in flow conditions upon addition of large flows of molecular substrate ($C_2H_xCl_y$). [e] Error limits represent statistical uncertainties and are reported as 2σ. Maximum estimated systematic uncertainties are 8% of the rate constant value (see text). [f] CH_3CCl_3 sample obtained from I. C. I. Chemicals and Polymers, Ltd. was used. CH_3CCl_3 sample obtained from Aldrich was used in all other experiments on reaction 4 (see discussion of impurities in section II).

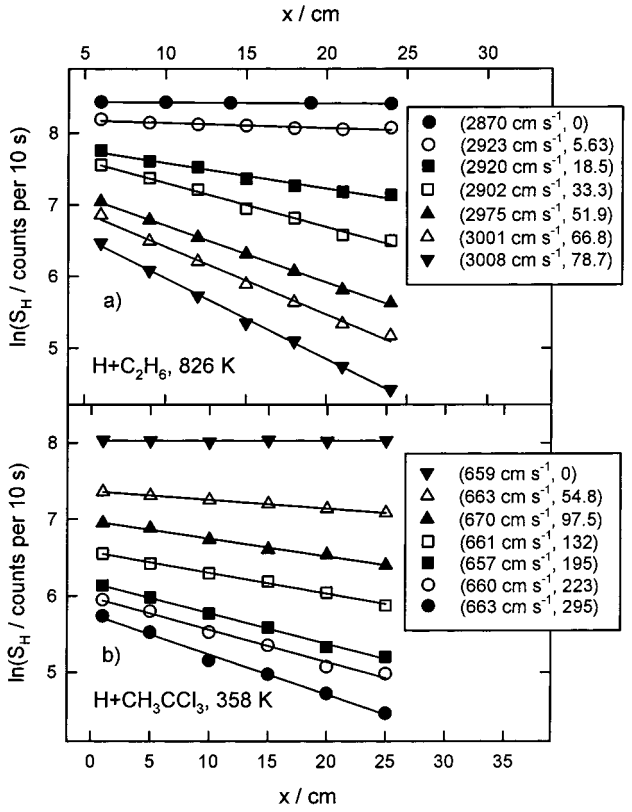

Figure 1. Examples of experimentally obtained $\ln(S_H)$ vs x dependences. Data from experiments 1−13 and 4−1 (see Table 1). Numbers in parentheses are the flow velocities and concentrations of $C_2H_xCl_y$ substrate (in 10^{13} molecules cm^{-3}).

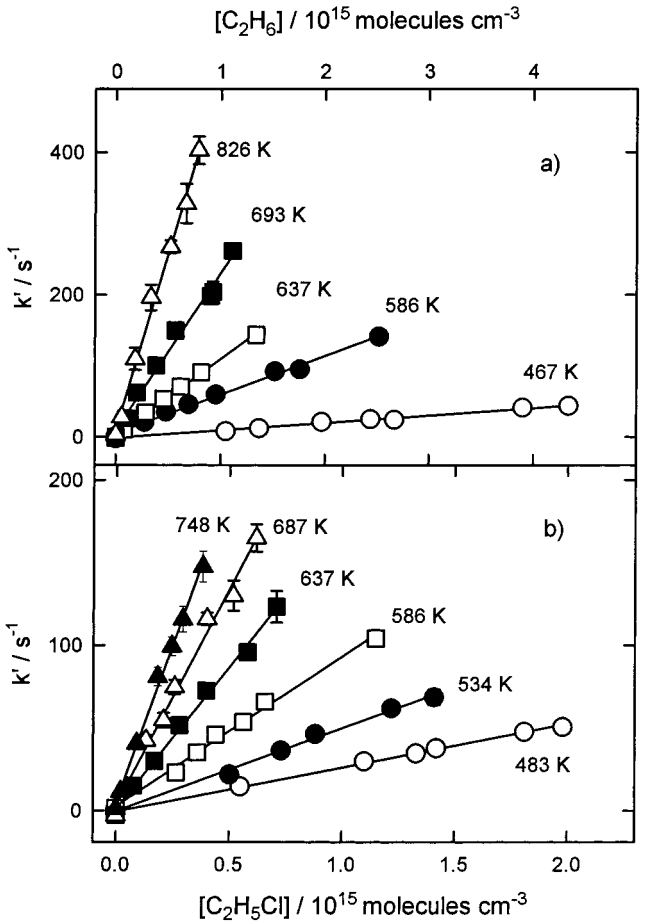

Figure 2. Examples of experimentally obtained k' vs $[C_2H_6]$ (a) and k' vs $[C_2H_5Cl]$ (b) dependences. Experimental temperatures are indicated on the plots.

k'_{OBS} were corrected for axial and radial diffusion of H atoms via the formula[24,26,33]

$$k' = k'_{OBS}\left(1 + \frac{k'_{OBS}D}{V^2} + \frac{k'_{OBS}R^2}{48D}\right) \qquad \text{(II)}$$

where D is the diffusion coefficient of H atoms in He and R is the reactor radius. The values of D were taken from the

$$D = 1.790\ (T/273\ \text{K})^{1.77}\ \text{cm}^2\ \text{s}^{-1}\ (P = 1\ \text{atm}) \qquad \text{(III)}$$

dependence derived by Krasnoperov et al.[34] based on the results of experiments and calculations reported in refs 35, 36, and 37. This correction for axial diffusion never exceeded 20% of the final value of k'.

The bimolecular rate constants of reactions 1−4 were obtained from the slopes of the linear dependences of k' on the concentration of substrate, $[C_2H_xCl_y]$

$$k' = k_i\,[C_2H_xCl_y] + k_0 \qquad \text{(IV)}$$

Here, k_i is the bimolecular rate constant of the reaction under study ($i = 1-4$) and k_0 is the zero-abscissa intercept of the k' vs $[C_2H_xCl_y]$ dependence. The k_0 intercept appears due to the nonnegligible losses of H atoms on the surfaces of the reactor and the movable injector and can acquire both positive and negative values.[15] The values of k_0 obtained in the current study were minor compared with the first term in eq IV (see Table 1) and uncertainties in k_0 were comparable with the k_0 values. Examples of experimentally obtained k' vs $[C_2H_xCl_y]$ dependences are presented in Figures 2 and 3.

Gases used in the experiments were obtained from MG Industries (He, >99.999%), Aldrich (C_2H_5Cl, > 99.7%; 1,2-$C_2H_4Cl_2$, 99.8%; CH_3CCl_3, 99.5%), and Matheson (C_2H_6, 99.999%; O_2 > 99.6%). An additional sample of CH_3CCl_3 was also obtained from I. C. I. Chemicals and Polymers, Ltd. Gas chromatographic analysis (subsection II.3) of this sample indicated a purity of 99.96%. All gases except helium were purified by vacuum distillation prior to use. Helium was purified by passing through liquid nitrogen cooled traps. A discussion of impurities and their potential influence on the experimental results is given in the next subsection (II.3).

II.3. Results. Conditions and results of experiments to determine the values of the rate constants of reactions 1−4 are presented in Table 1. The rate constants demonstrate no dependence on pressure or initial concentration of H atoms within the experimental ranges. The observed pressure independence is anticipated because the mechanisms of reactions 1−4 are expected to be those of atom abstraction. The fact that the rate constants are independent of the initial H atom concentration indicates the absence of any influence of potential secondary reactions on the kinetics of H atoms, as can be expected due to the low values of $[H]_0$ used ($[H]_0 = (2.2-8.4) \times 10^{10}$ atoms cm^{-3}).

Heterogeneous reactions of H atoms with the $C_2H_xCl_y$ substrate adsorbed on the reactor wall could potentially influence the observed rate of H atom decay, k'. If adsorption of substrate is saturated, this effect would be manifested only by positive values of k_0 and the obtained k_i values would not be affected. If, however, the adsorption is not saturated but increases with the concentration of substrate, the contribution of such a heterogeneous reaction can influence the slope of the k' vs $[C_2H_x$-

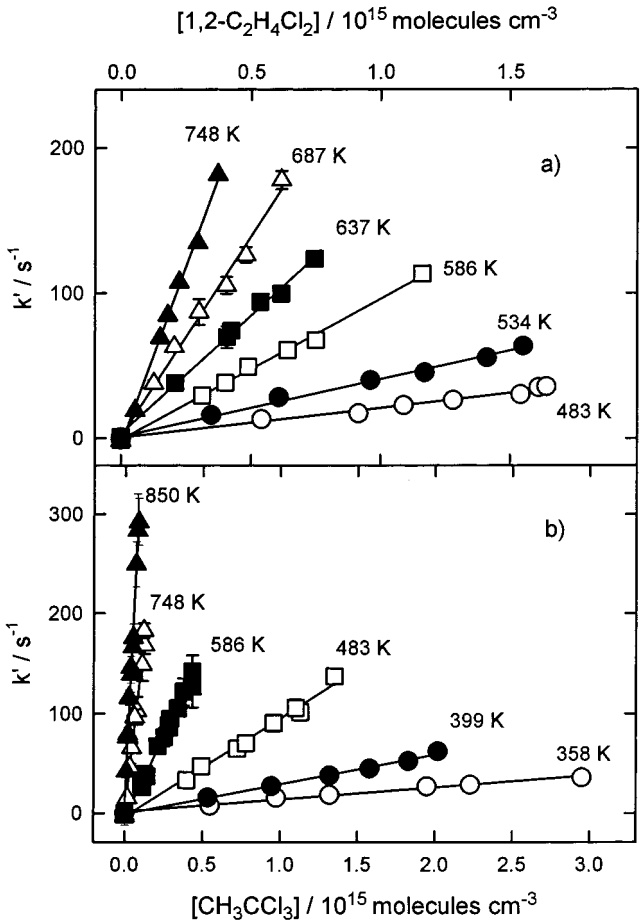

Figure 3. Examples of experimentally obtained k' vs [1,2-$C_2H_4Cl_2$] (a) and k' vs [CH_3CCl_3] (b) dependences. Experimental temperatures are indicated on the plots.

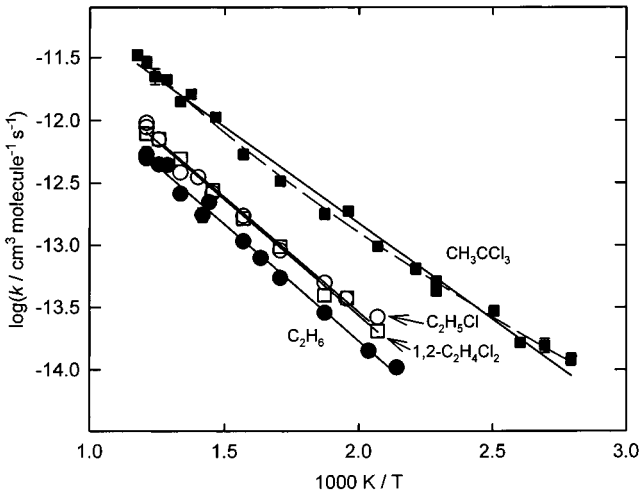

Figure 4. Experimental temperature dependences of the rate constants of reactions 1−4. Symbols are experimental data points: filled circles, reaction 1; open circles, reaction 2; open squares, reaction 3; filled squares, reaction 4. Solid lines are Arrhenius fits of data obtained in the current work, formulas V−VIII. Dashed line is the modified Arrhenius fit given by formula IX.

Cl_y] dependence. In this case, there are two possibilities. First, the dependence of the surface density of substrate on its concentration in the gas phase is nonlinear and thus any hypothetical heterogeneous component to the observed H atom decay rate would exhibit a nonlinear dependence on [$C_2H_xCl_y$]. Alternatively, if the density of the adsorbed substrate increases linearly with its gas-phase concentration, the observed k' vs [$C_2H_xCl_y$] dependences are expected to be linear, as in the case of a purely gas-phase reaction.

To ensure that the measured rates of H atom decay in the presence of $C_2H_xCl_y$ represent the homogeneous reactions 1−4, experiments were conducted with reactors of different internal diameters (1.93−4.66 cm) possessing different surface-to-volume ratios. The experimentally obtained values of the rate constants were independent of the reactor used (Table 1). This independence, as well as the linearity of the observed k' vs [$C_2H_xCl_y$] dependences, indicates the absence of any significant effects of heterogeneous reactions on the values of the rate constants.

The rate constants of reactions 1−4 exhibit positive temperature dependences (Figure 4) that can be represented with Arrhenius expressions within their corresponding experimental temperature ranges

$$k_1 = (9.5 \pm 3.7) \times 10^{-11}\exp(-4316 \pm 212\ \mathrm{K/T})$$
$$\mathrm{cm^3\ molecule^{-1}\ s^{-1}}\ (467-826\ \mathrm{K}) \quad \text{(V)}$$

$$k_2 = (1.21 \pm 0.60) \times 10^{-10}\exp(-4146 \pm 258\ \mathrm{K/T})$$
$$\mathrm{cm^3\ molecule^{-1}\ s^{-1}}\ (483-826\ \mathrm{K}) \quad \text{(VI)}$$

$$k_3 = (1.45 \pm 0.48) \times 10^{-10}\exp(-4290 \pm 183\ \mathrm{K/T})$$
$$\mathrm{cm^3\ molecule^{-1}\ s^{-1}}\ (483-826\ \mathrm{K}) \quad \text{(VII)}$$

$$k_4 = (1.83 \pm 0.62) \times 10^{-10}\exp(-3552 \pm 153\ \mathrm{K/T})$$
$$\mathrm{cm^3\ molecule^{-1}\ s^{-1}}\ (358-850\ \mathrm{K}) \quad \text{(VIII)}$$

The temperature dependence of the rate constant of reaction 4 can also be represented with a modified Arrhenius expression

$$k_4 = 5.94 \times 10^{-24}\, T^{4.23} \exp(-1249\ \mathrm{K}/T)$$
$$\mathrm{cm^3\ molecule^{-1}\ s^{-1}}\ (358-850\ \mathrm{K}) \quad \text{(IX)}$$

which reflects the curvature observed in the $\log(k_4)$ vs $1/T$ dependence. However, the power of the T parameter (4.23 ± 1.72) has a rather large uncertainty, which prevents any certain conclusion regarding the extent of the curvature. The error limits of the parameters in expressions V−IX represent uncertainties of the fits only and are reported as 2σ. Error limits of the "preexponential factor" and "activation energy" parameters in expression IX are not presented here as these parameters bear no physical meaning.

The lowest temperatures used were determined by the impracticality of measuring rate constants that are lower than 10^{-14} cm^3 $molecule^{-1}$ s^{-1}. The upper limits of the experimental temperature ranges for reactions 1, 2, and 4 were determined by the onset of thermal decomposition of radical products. These decomposition reactions resulted in the regeneration of H atoms and consequent nonlinearity of the $\ln(S_H)$ vs x kinetic dependences (see formula I).

The sources of error in the measured experimental parameters such as temperature, pressure, flow rate, signal count, and so forth were subdivided into statistical and systematic. Statistical uncertainties were estimated for parameters statistical in physical nature (for example, signal count). The estimate of possible systematic errors was based on the finite accuracy of the equipment and on the uncertainty in the H atom diffusion coefficient.[34] The uncertainties of the measured experimental parameters were propagated to the final values of the rate constants using different mathematical procedures for propagat-

ing systematic and statistical uncertainties.[38] The error limits of the experimentally obtained values reported in this work (Table 1) represent 2σ statistical uncertainty. Maximum estimated systematic uncertainty is 8% of rate constant value.

To verify that no potential impurities in the chlorinated ethanes could affect the measured rate constants, these gases were analyzed for potential contaminants by gas chromatography. A Shimadzu GC-9A gas chromatograph was used in these analyses. It was found that, after purification by vacuum distillation, the purity of all chloroethanes (C_2H_5Cl, >99.98%; 1,2-$C_2H_4Cl_2$, >99.99%; CH_3CCl_3, >99.997% (sample obtained from Aldrich)) significantly exceeded the specifications provided by the manufacturers. The impurities that are most likely to be found in the chloroethanes are the corresponding chlorinated ethylenes (for example, C_2H_3Cl as an impurity in C_2H_5Cl). The rate constants of the reactions of H atoms with chlorinated ethylenes can be expected to be lower than 10^{-11} cm^3 molecule s^{-1}. For example, the temperature dependence of the high-pressure-limit rate constant obtained by Knyazev et al.[39] in their experiment-based modeling of the $H + C_2H_3Cl \leftrightarrow CH_3CHCl$ reaction results in a rate constant of 5.8×10^{-12} cm^3 molecule s^{-1} at 483 K, the lowest experimental temperature used in the current study of the $H + C_2H_5Cl$ reaction. This value is further reduced to 1.7×10^{-12} cm^3 molecule s^{-1} by falloff effects at the experimental pressure of 4 Torr. Thus, a 0.02% impurity of vinyl chloride in chloroethane will result in a contribution of 3.4×10^{-16} cm^3 molecule s^{-1} to the measured rate constant of reaction 2, or 1.3% at this temperature. The potential effects of impurities are expected to decrease with temperature since the activation energies of the reactions of addition to a double bond are less than those of H or Cl atom abstraction. Therefore, impurity effects on the values of the rate constants obtained in the current study are negligible compared to the experimental uncertainties.

The sample of CH_3CCl_3 obtained from Aldrich was stabilized with a minor fraction of low alkyl epoxides, as stated by the manufacturer. To ensure that the presence of the stabilizer in the sample had no influence on the determined rate constants, additional experiments were conducted with a sample of CH_3CCl_3 obtained from I. C. I. Chemicals and Polymers, Ltd., which did not contain the stabilizer. Gas chromatographic analysis of this second sample of 1,1,1-trichloroethane revealed the presence of ~0.03% of impurity. The experimental rate constant values of reaction 4 did not vary with the source of CH_3CCl_3 (Table 1), thus indicating the absence of any measurable impurity effects.

III. Transition State Theory Model of Reaction 1

Although the rate constants of reactions 1−4 were obtained experimentally over wide temperature ranges, accurate extrapolation to lower and higher temperatures is still needed. The reactions of H atoms with chlorinated ethanes can proceed through the abstraction of both chlorine and hydrogen atoms and the relative importance of these two types of processes is unknown. Thus, modeling-based extrapolation of experimental rate constants is restricted here to reaction 1 ($H + C_2H_6$) where only the hydrogen atom abstraction is possible.

Modeling is performed using the approach applied by us earlier to the reactions of H atoms with methane and chlorinated methanes.[15] Initial approximation to the properties of the reaction transition state (geometry and vibrational frequencies) was obtained in ab initio calculations using the UMP2/6-31G(d,p) method. Vibrational frequencies were scaled by a factor of 0.9427.[40] Rate constant values were calculated using the classical transition state theory formula (see, for example, ref 41). A final adjustment of the six frequencies representing the bending deformations of the $CH_3CH_2\cdots H\cdots H$ transitional structure and of the reaction barrier height was performed to reproduce the experimental temperature dependence of the rate constant. Experimental values of k_1 obtained in this work and those reported by Jones, Morgan, and Purnell[22] (see section III, "Discussion") were used in the fitting of the model parameters. Adjustment of frequencies was performed by a multiplication by a uniform factor.

Tunneling can be expected to play a significant role in reaction 1 at low temperatures. Therefore, extrapolation to low temperatures must be accompanied by estimates of the uncertainties associated with the contribution of tunneling. Computation of the quantum tunneling correction performed in this work was based on the knowledge of the barrier "width" parameter.[15,42,43] The shape of the reaction potential energy barrier was determined using the method of reaction path following (intrinsic reaction coordinate, IRC)[44,45] in mass-weighted internal coordinates. The resultant barrier potential energy profiles were fitted with the Eckart function[46]

$$V = \frac{A\xi}{(1+\xi)} + \frac{B\xi}{(1+\xi)^2}; \quad \xi = \exp\left(\frac{2\pi x}{l}\right) \qquad \text{(X)}$$

to determine the "width" parameter l which was used in the calculation of the tunneling correction. The method of computing the tunneling probabilities based on the determination of the barrier "width" parameter from quantum chemical calculations results in the decoupling of the width and the height of the reaction barrier. When the latter is adjusted in the fitting of experimental data, the barrier curvature and the associated imaginary frequency changes accordingly. This makes the current method more accurate than the often used approach where the imaginary frequency is obtained from ab initio calculations but its change due to further barrier adjustment is neglected. Reference 15 can be consulted for details of the computational approach.

Several computational methods of quantum chemistry were used in the IRC calculations: UMP2/6-31G(d,p), B3LYP with the 6-311G(2d,2p) and 6-311+G(2d,2p) basis sets, and G2 and QCISD(T)/6-311+G(2d,2p) single-point energy calculations along the IRC computed at the UMP2/6-31G(d,p) level. Ref 47 can be consulted for the description of the methods and the basis sets used. The G2 calculations resulted in an unrealistic potential energy profile characterized by two maxima instead of one, which was discarded as an artifact. IRC calculations performed with other methods resulted in barrier shapes which could not be well fitted with the Eckart function. Considering that it is the top part of the barrier that plays the most significant role in the tunneling effect, it is more important to describe this upper portion with the Eckart equation than the barrier as a whole. Thus, we limited the fitting attempts to the top one-third and the top one tenth of the barrier, where the quality of fits was acceptable. Although the computed barrier heights (relative to $H + C_2H_6$) differ from method to method (87 kJ mol^{-1} at the UMP2/6-31G(d,p) level, 52 kJ mol^{-1} at the QCISD(T)/6-311+G(2d,2p)//UMP2/6-31G(d,p) level, and 28 and 29 kJ mol^{-1} at the B3LYP/6-311+G(2d,2p) and the B3LYP/6-311G(2d,2p) levels, respectively), the "width" parameter values obtained with different methods are remarkably similar. Table 2 lists the values of the barrier "width" parameter l obtained in the calculations. The observed very weak dependence of the barrier "width" parameter on the computational level is in agreement with similar findings of earlier studies[15,42,43] where the barrier width-based method of accounting for tunneling was

TABLE 2: Values of the Reaction "Barrier Width" Parameter (l) for the H + C_2H_6 ↔ H_2 + C_2H_5 Reaction Obtained in the IRC Following Calculations

			l/amu$^{1/2}$ Å	
method[a]	barrier height[b]	ΔE[c]	top 1/3[d]	top 1/10[e]
UMP2/6-31G(d,p)	86.7	26.6	1.328	1.200
QCISD(T)/6-311+G(2d,2p)//UMP2/6-31G(d,p)[f]	52.3	−3.5	1.341	1.278
B3LYP/6-311+G(2d,2p)	28.5	−15.7	1.287	1.208
B3LYP/6-311G(2d,2p)	28.8	−12.6	1.297	1.195
average			1.313	1.220

[a] Computational method used in IRC following. [b] Barrier height relative to reactants. Units are kJ mol^{-1}. [c] Energy of products minus energy of reactants. Units are kJ mol^{-1}. [d] Values of the l barrier "width" parameter obtained in fitting of the top one-third of the barrier (relative to the higher of the energies of reactants or products, depending on the computational method). [e] Values of the l barrier "width" parameter obtained in fitting of the top one tenth of the barrier (relative to the higher of the energies of reactants or products, depending on the computational method). [f] A series of single-point QCISD(T)/6-311+G(2d,2p) energy calculations performed for structures along the UMP2/6-31G(d,p)-level IRC.

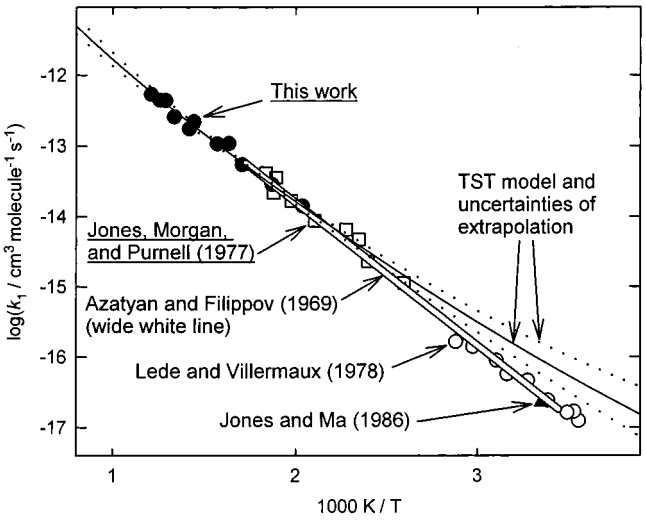

Figure 5. Plot of the rate constants of reaction 1 (H + C_2H_6→H_2 + C_2H_5). Experimental data: (filled circles) k_1 values obtained in the current study; (open squares) k_1 values of Jones, Morgan, and Purnell;[22] (wide white line) k_1 vs T dependence reported by Azatyan and Filippov;[20] (open circles) k_1 from Lede and Villermaux;[21] (filled triangle) room-temperature k_1 value reported by Jones and Ma.[23] References to the two experimental determinations free of influences from secondary reactions (no stoichiometric corrections were needed) are underlined. Solid thin line: extrapolation of the experimental data obtained in the current study and in ref 22 with the transition state theory model. Dotted lines: uncertainties of extrapolation arising from the scatter of the experimental data and from the treatment of tunneling.

used. Such a virtual absence of dependence upon the computational method is expected because l is, essentially, a geometrical parameter and, as such, can be expected to be determined with reasonable accuracy by relatively low-level ab initio methods. In the transition state theory model of reaction 1, the average of the l values obtained from fitting the top one-third of the barrier was used (l = 1.313 amu$^{1/2}$ Å) and uncertainties in the determination of l were taken into account (vide infra).

The above model of reaction 1 results in a temperature dependence of the rate constant that can be represented by the following expressions (solid line in Figure 5)

$$k_1(T) = 4.45 \times 10^{-17} T^{1.98} \exp(-3183\ \mathrm{K}/T)$$
$$\mathrm{cm^3\ molecule^{-1}\ s^{-1}},\ T = 300-3000\ \mathrm{K}\ (8\%) \quad \text{(XI)}$$

$$k_1(T) = 3.72 \times 10^{-40} T^{9.72} \exp(-467\ \mathrm{K}/T)$$
$$\mathrm{cm^3\ molecule^{-1}\ s^{-1}},\ T = 200-400\ \mathrm{K}\ (7\%) \quad \text{(XII)}$$

Different formulas are provided for the low and the high-temperature regions since the whole 200−3000 K temperature range cannot be described with one modified Arrhenius expression. The percentage values given in parentheses indicate the maximum deviations between the calculated values and the expressions XI and XII. The same model results in a temperature dependence of the rate constant of the reverse reaction, C_2H_5 + H_2 → H + C_2H_6

$$k_{-1}(T) = 2.27 \times 10^{-20} T^{2.43} \exp(-4444\ \mathrm{K}/T)$$
$$\mathrm{cm^3\ molecule^{-1}\ s^{-1}},\ T = 300-3000\ \mathrm{K}\ (3\%) \quad \text{(XIII)}$$

$$k_{-1}(T) = 1.19 \times 10^{-39} T^{8.94} \exp(-2267\ \mathrm{K}/T)$$
$$\mathrm{cm^3\ molecule^{-1}\ s^{-1}},\ T = 200-400\ \mathrm{K}\ (2\%) \quad \text{(XIV)}$$

The differences between the l values obtained with different computational methods are smaller than the differences between the results of fitting the top one-third and the top one tenth of the barrier (Table 2). Uncertainties of the model associated with the description of tunneling were estimated by repeating the modeling (including the fitting of experimental rate constant data) with the l parameter incremented in both the "plus" and the "minus" directions by twice the difference between the "one-third" and "one-tenth" values: l_{min} = 1.127 and l_{max} = 1.499 amu$^{1/2}$ Å.

An additional uncertainty of the model is due to the experimental uncertainties of the rate constant values. The uncertainty arising from the experimental data scatter was estimated by extrapolating the combined set of the $k_1(T)$ values obtained in the current study and in the work of Jones, Morgan, and Purnell[22] from the "center of mass" of the experimental temperature interval (T_c = 558 K) and calculating the deviations resulting from the use of the maximum and the minimum values (central value ± 2σ) of the activation energy and the rate constant at $T = T_c$. The overall uncertainties of the model (dotted lines in Figure 5) were obtained by multiplying the tunneling and the experimental extrapolation uncertainty factors. Thus, the estimated overall uncertainty factor reaches the values of 6 (upper limit) and 4(lower limit) at 200 K, 1.7 at 300 K, 1.2 at 400 and 1000 K, 1.5 at 2000 K, and 1.6 at 3000 K.

The results of the ab initio calculations, the shapes of the reaction barrier, and the fitted Eckart function parameters are presented in the Supplement. The details of the final model of reaction 1 are given in Table 3.

IV. Discussion

The current study provides the first direct determination of the temperature dependences of the rate constants of reactions 2−4. Reaction 1, that of H atoms with ethane, has been studied before by numerous groups. Reviews of literature can be found elsewhere.[17−19] However, only in four studies was the rate of

TABLE 3: Properties of Molecules and the Transition State Used in the Models of Reaction 1

vibrational frequencies and degeneracies (cm^{-1}):

C_2H_6:[50]	2953.7 (1), 1388.4 (1), 994.8 (1), 2895.8 (1), 1379.2 (1), 2985.4 (2), 1471.4 (2), 821.6 (2), 2968.7 (2), 1468.1 (2), 1190 (2)
C_2H_5:[a]	3114, 3036, 2987, 2920, 2844, 1442, 1442, 1383, 1369, 1133, 1185, 1025, 783, 532
H_2:[51]	4162
H···H···C_2H_5:[b]	645 [561], 975 [848], 1358 [1181], 1366 [1187], 345 [300], 1389 [1208], 809, 1009, 1096, 1377, 1444, 1464, 1465, 1720, 2943, 3014, 3024, 3046, 3105

rotational constants (cm^{-1}), symmetry no.s, and torsional barrier:

C_2H_6:[50]	overall rotation:	$B = 1.0550$	$\sigma = 6$	
	internal rotation:	$B = 10.684$	$\sigma = 3$	$V_0 = 1024\ cm^{-1}$
C_2H_5:	overall rotation:	$B = 1.2256$	$\sigma = 1$	
	internal rotation:	$B = 15.187$	$\sigma = 6$	
H_2:		$B = 59.3444$	$\sigma = 2$	
H···H···C_2H_5:[c]	overall rotation:	$B = 0.7999$	$\sigma = 1$	
	internal rotation:	$B = 7.550$	$\sigma = 3$	$V_0 = 907\ cm^{-1}$

reaction energy barriers:

$E_1 = 38.27\ kJ\ mol^{-1}$ $E_{-1} = 53.83\ kJ\ mol^{-1}$

imaginary frequency (cm^{-1}):[d]

$\upsilon_i = 1206i\ cm^{-1}$

[a] Properties of C_2H_5 are a combination of the experimental data of Chettur and Snelson[52] and the ab initio results of Quelch et al.[53] [b] Vibrational frequencies of the transition state were obtained in UMP2/6-31G(d,p)-level ab initio calculations and scaled[40] by 0.9427. Frequencies of six transitional modes were adjusted via multiplication by a uniform factor (see text, section III). Numbers in square brackets are the original (unadjusted) scaled ab initio values. [c] Geometry of the transition state and the torsional barrier (which includes ZPVE correction) were calculated at the UMP2/6-31G(d,p) level. [d] The imaginary frequency was obtained from the barrier "width" parameter ($l = 1.313\ amu^{1/2}$ Å) and the fitted value of the barrier height.

reaction 1 measured directly by monitoring kinetics of at least one of the reactants.[20−23] Each of these four studies utilized the discharge flow technique. Azatyan and Filippov[20] used ESR detection of hydrogen atoms and determined the rate constant of reaction 1 in the 290−579 K temperature range. Lede and Villermaux[21] applied the H atom detection method based on the reaction of H with HgO and subsequent spectrophotometric detection of Hg product at 253.7 nm. These authors reported the rate constants of reaction 1 between 281 and 347 K. Jones, Morgan, and Purnell[22] used mass spectrometry to detect H atoms and C_2H_6 and obtained values of k_1 at $T = 385-544$ K. Finally, Jones and Ma[28] used ESR to detect H atoms and reported a k_1 value at room temperature. The values of k_1 reported by these four groups are presented in Figure 5 together with the results of the current study.

H atom concentrations used in these four studies of reaction 1 were relatively high, $[H]_0 \approx 10^{12}-10^{15}$ molecules cm^{-3}. As a result, more than one atom of hydrogen was consumed per each act of the H + C_2H_6 reaction. The authors of refs 20 and 21 divided the apparent values of the rate constant obtained from their experiments by the assumed stoichiometric factor of 4, which was derived from the following sequence of reactions

$$H + C_2H_6 \rightarrow H_2 + C_2H_5 \quad (1)$$

$$H + C_2H_5 \rightarrow 2\ CH_3 \quad (5)$$

$$H + CH_3 \rightarrow CH_4 \quad (6)$$

Jones and Ma[28] did not apply any stoichiometric factor to their results, although the high initial concentrations of H atoms used ($10^{12}-10^{13}$ molecules cm^{-3}, estimated here on the basis of the values of gas flows and calibration data reported in ref 28) warranted such a correction for the fast secondary reactions 5 and 6. Thus, the agreement between their reported rate constant value at room temperature and those of other groups (Figure 5) is rather superficial.

The only previous experimental study of reaction 1 where no stoichiometric correction was required was that of Jones, Morgan, and Purnell.[22] These authors conducted experiments in an excess of H atoms over C_2H_6 (pseudo-first-order conditions for C_2H_6) and monitored the kinetics of the disappearance of the latter to obtain the values of k_1. Additional experiments were performed in an excess of C_2H_6 and comparison of the results with those obtained under the conditions of excess of H yielded the values of the stoichiometric correction factor as a function of temperature. It was found that this factor changed from 3.7 at 385 K to 1.8 at 540 K, which challenges the validity of the other groups' use of the assumed universal value of four. Therefore, the work of Jones, Morgan, and Purnell[22] is the only one among previous studies of the H + C_2H_6 reaction that provided accurate values of k_1, free of uncertainties associated with the contributions from secondary chemistry.

Figure 5 displays the experimental temperature dependence of k_1 obtained in this work in comparison with earlier determinations.[20−23] The results of the current study (obtained under conditions where secondary reactions are negligible) are in agreement with those of ref 22. A combined set of the $k_1(T)$ values obtained in the current study and in the work of Jones, Morgan, and Purnell[22] results in the following Arrhenius dependence

$$k_1(T) = (1.04 \pm 0.4) \times 10^{-10} \exp((-4357 \pm 191\ K)/T)\ cm^3\ molecule^{-1}\ s^{-1} \quad (XV)$$

(Error limits are 2σ and represent the statistical uncertainties of the fit only).

Extrapolation to lower temperatures via the model described in section II (solid thin line) yields rate constant values that are larger than the experimental values of Azatyan and Filippov[20] and Lede and Villermaux.[21] The lower limit of the estimated uncertainties is still approximately a factor of 1.5−2.0 higher than these experimental data.[20,21] This deviation can be explained if one supposes that the factor of 4 stoichiometric correction

used by these groups[20,21] was somewhat overestimated. If the values of refs 20 and 21 are combined with the results of ref 22 and those of the current study, the resultant $k_1(T)$ Arrhenius plot becomes linear. Such linearity, however, does not appear to be realistic since some low-temperature curvature can be expected due to tunneling.

The sequence of reactions 1, 5, and 6 which led the authors of refs 20 and 21 to use the universal stoichiometric correction factor of 4 neglects the potential influence of reaction

$$C_2H_5 + CH_3 \rightarrow n\text{-}C_3H_8 \qquad (7)$$

$$\rightarrow C_2H_4 + CH_4$$

The rate constant of reaction 7 (the sum of the two channels) at room temperature is 9.8×10^{-11}, as measured recently by Knyazev and Slagle.[54] Reaction 7 will compete with reactions 5 and 6 and thus will reduce the effective stoichiometric factor. The value of the stoichiometric factor can be expected to depend on pressure (due to the pressure dependence of the rate constant of reaction 6), the initial concentrations of H and C_2H_6, and on the heterogeneous wall losses of radicals. These radical wall losses are, most likely, negligible under the conditions of ref 21 due to the high pressure (90−403 Torr) and slow diffusion but could be a factor under the conditions of ref 20 (pressure of 4 Torr). Kinetic modeling performed in the current work for the typical conditions of ref 21 ($T = 300$ K, $[H]_0 = 6 \times 10^{12}$ atom cm^{-3}, $[C_2H_6] = 3.8 \times 10^{17}$ molecules cm^{-3}, $P = 300$ Torr, reaction time 30−80 ms) with reactions 1, 5, 6, and 7, as well as the recombination of CH_3 included in the model resulted in the stoichiometric factor of 3.1. In these calculations, the following values of the rate constants were used: $k_1 = 3.5 \times 10^{-17}$, $k_5 = 6 \times 10^{-11}$,[17] $k_6 = 1.35 \times 10^{-10}$ (estimated from the plot of pressure dependence in ref 17), $k_7 = 9.8 \times 10^{-11}$,[54] $k(2CH_3 \rightarrow C_2H_6) = 6 \times 10^{-11}$ cm^3 molecule^{-1} s^{-1}.[17] The calculation of the stoichiometric factor for the conditions of Azatyan and Filippov[20] is complicated due to the absence of data on the initial concentrations of H. The values of 3.9 and 3.4 are obtained for room-temperature conditions using the values of $[H]_0 = 10^{14}$ and 10^{13} atom cm^{-3}, respectively. Moreover, at the upper end of the experimental temperature range of ref 20 (579 K) the estimated stoichiometric factor becomes 1.4 (in reasonable agreement with the value of 1.8 at 540 K determined in ref 22) instead of the value of 4.0 used by Azatyan and Filippov[20] and thus the agreement between the high-temperature results of ref 20 and those of ref 22 and the current work disappears.

The above discussion serves to emphasize the uncertainties associated with the experimental values of k_1 at low temperatures. On the other hand, the extrapolation of the results of the current study and ref 22 to lower temperatures is also characterized by significant uncertainties, as discussed in section III. In particular, the treatment of tunneling is based on a one-dimensional Eckart approximation, the validity of which has not been established in any rigorous way for chemical reactions of polyatomic species. The reliability of the extrapolation also depends on the accuracy of the k_1 values reported in both the current experimental study and that of Jones, Morgan, and Purnell.[22] These additional factors contributing to uncertainty are not easily quantified and thus are not included in the estimates of the uncertainty of extrapolation in section III. The only conclusion that can be reached on the basis of this discussion is that the low-temperature values of the rate constant of reaction 1 remain uncertain.

The only previous measurement of the rate constant of reaction 2, that of H atom with chloroethane, was performed by Triebert et al.[16] by the discharge flow method with mass spectrometric detection of C_2H_5Cl. Experiments were conducted in an excess of H atoms. The k_2 reported in ref 16 is significantly higher than the value obtained by an Arrhenius extrapolation of the results of the current study to lower temperatures (Figure 6). The difference reaches an order of magnitude, which makes a potential explanation by non-Arrhenius curvature due to tunneling unlikely. It should be noted that in the work of Triebert et al. the concentration of H atoms was affected by a significant wall decay. The unknown rate constant of this decay was used by the authors as an additional adjustable parameter in the fitting of kinetic curves.

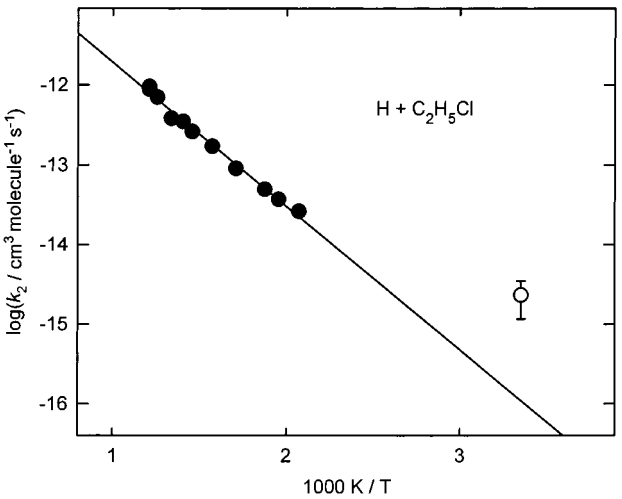

Figure 6. Temperature dependence of the rate constant of reaction 2 ($H + C_2H_5Cl \rightarrow$products). Filled circles, experimental data obtained in the current study. Open circle, the room-temperature value of Triebert et al.[16] Line: Arrhenius extrapolation of the rate constants obtained in the current study.

H atom attack on chlorinated ethanes can result in the abstraction of both Cl and H atoms. In our recent study of the reactions of H atoms with methane and chlorinated methanes, transition-state-theory modeling, an ab initio study of the properties of transition states, and the Marcus formula[48] describing the correlation between heats of reaction and reaction barriers were used to estimate the relative importance of the H- and the Cl-abstraction routes. In that study, unambiguous cases of abstraction of only H and only Cl atoms were provided by the reactions of H atoms with methane and CCl_4, respectively. The rate constants of Cl abstraction were obtained by subtracting the estimated H-abstraction contributions from the overall rates of the reactions of H atoms with chloromethanes. The resultant activation energies of the Cl abstraction reaction routes demonstrated a correlation with the reaction thermochemistry that can be described with the Marcus formula.[48] The systems considered in the current work, the reactions of H atoms with ethane and chlorinated ethanes, present a more complicated situation. More than one site of abstraction can be present in substituted ethanes (e.g., abstraction of an H atom in the primary vs secondary positions in C_2H_5Cl). No experimental thermochemical data are available on the radical products of the H abstraction channels in reactions 3 and 4, and the existing data on the heat of formation of CH_3CCl_2 (product of the Cl-abstracting channel in reaction 4) is rather uncertain.[49] For these reasons, and considering the absence of experimental rate data for the reactions of H atoms with other chlorinated ethanes, we do not attempt here a computational analysis directed at separation of the H and Cl abstraction routes in reactions 2−4.

Acknowledgment. This research was supported by the National Science Foundation, Combustion and Thermal Plasmas Program, under Grant No. CTS-9807136. The authors would like to thank Dr. L. J. Stief for helpful advice and the loan of equipment and Dr. V. L. Orkin for advice and help with the analyses of chloroethane samples.

Supporting Information Available: Supplement describing the results of the ab initio calculations of the transition state, reactants, and products of reaction 1 (11 pages). Table 1S containing information on the optimized geometries and energies of these species. Figures 1S−5S displaying the potential energy profiles along IRCs of reactions 1 at 5 different levels of calculation and the results of fitting with the Eckart formula.

References and Notes

(1) Karra, S. B.; Gutman, D.; Senkan, S. M. *Combust. Sci. Technol.* **1988**, *60*, 45.
(2) Chang, W. D.; Senkan, S. M. *Environ. Sci. Technol.* **1989**, *23*, 442.
(3) Lee, K. Y.; Yang, M. H.; Puri, I. K. *Combust. Flame* **1993**, *92*, 419.
(4) Wang, H.; Hahn, T. O.; Sung, C. J.; Law, C. K. *Combust. Flame* **1996**, *105*, 291.
(5) Chang, W. D.; Karra, S. B.; Senkan, S. M. *Combust. Sci. Technol.* **1986**, *49*, 107.
(6) Karra, S. B.; Senkan, S. M. *Combust. Sci. Technol.* **1987**, *54*, 333.
(7) Xieqi, M.; Cicek, B.; Senkan, S. M. *Combust. Flame* **1993**, *94*, 131.
(8) Cicek, B.; Senkan, S. M. *Combust. Sci. Technol.* **1993**, *91*, 53.
(9) Cui, J. P.; He, Y. Z.; Tsang, W. *J. Phys. Chem.* **1989**, *93*, 724.
(10) Lee, K. Y.; Puri, I. K. *Combust. Flame* **1993**, *92*, 440.
(11) Lee, K. Y.; Puri, I. K. *Combust. Flame* **1993**, *94*, 191.
(12) Taylor, P. H.; Tirey, D. A.; Dellinger, B. *Combust. Flame* **1996**, *104*, 260.
(13) Taylor, P. H.; Tirey, D. A.; Dellinger, B. *Combust. Flame* **1996**, *106*, 1.
(14) Ho, W. P.; Yu, Q.-R.; Bozzelli, J. W. *Combust. Sci. Technol.* **1992**, *85*, 23.
(15) Bryukov, M. G.; Slagle, I. R.; Knyazev, V. D. *J. Phys. Chem. A.* **2001**, *105*, 3107.
(16) Triebert, J.; Meinike, T.; Olzmann, M.; Scherzer, K. *Z. Phys. Chem. (Munich)* **1995**, *191*, 47.
(17) Baulch, D. L.; Cobos, C. J.; Cox, R. A.; Esser, C.; Frank, P.; Just, Th.; Kerr, J. A.; Pilling, M. J.; Troe, J.; Walker, R. W.; Warnatz, J. *J. Phys. Chem. Ref. Data* **1992**, *21*, 411.
(18) Tsang, W.; Hampson, R. F. *J. Phys. Chem. Ref. Data* **1986**, *15*, 1087.
(19) Camilleri, P.; Marshall, R. M.; Purnell, J. H. *J. Chem. Soc., Faraday Trans. 1* **1974**, *70*, 1434.
(20) Azatyan, V. V.; Filippov, S. B. *Dokl. Phys. Chem. (Engl. Transl.)* **1969**, *184*, 49.
(21) Lede, J.; Villermaux, J. *Can. J. Chem.* **1978**, *56*, 392.
(22) Jones, D.; Morgan, P. A.; Purnell, J. H. *J. Chem. Soc., Faraday Trans. 1* **1977**, *73*, 1311.
(23) Jones, W. E.; Ma, J. L. *Can. J. Chem.* **1986**, *64*, 2192.
(24) Kaufman, F. *Prog. React. Kinet.* **1961**, *1*, 1.
(25) Poirier, R. V.; Carr, R. W. *J. Phys. Chem.* **1971**, *75*, 1593.
(26) Howard, C. J. *J. Phys. Chem.* **1979**, *83*, 3.
(27) Ogren, P. J. *J. Phys. Chem.* **1975**, *79*, 1749.
(28) Sepehrad, A.; Marshall, R. M.; Purnell, H. *Int. J. Chem. Kinet.* **1979**, *11*, 411.
(29) Davis, D. D.; Braun, W. *Appl. Opt.* **1968**, *7*, 2071.
(30) Okabe, H. *Photochemistry of Small Molecules.*; Wiley: New York, 1978.
(31) Kurylo, M. J.; Peterson, N. C.; Braun, W. *J. Chem. Phys.* **1970**, *53*, 2776.
(32) Tsang, W.; Herron, J. T. *J. Phys. Chem. Ref. Data* **1991**, *20*, 609.
(33) Lambert, M.; Sadowski, C. M.; Carrington, T. *Int. J. Chem. Kinet.* **1985**, *17*, 685.
(34) Krasnoperov, L. N.; Kalinovski, I. J.; Chu, H.-N.; Gutman, D. *J. Phys. Chem.* **1993**, *97*, 11 787.
(35) Kartoshkin, V. A.; Klementev, G. V.; Melnikov, V. D. *Opt. Spektrosk.* **1983**, *55*, 606.
(36) Zelenov, V. V.; Kukui, A. S.; Dodonov, A. F. *Khim Fiz.* **1986**, *5*, 702.
(37) Redsun, S. G.; Knize, R. J. *Phys. Rev. A* **1988**, *37*, 737.
(38) Bevington, P. R. *Data Reduction and Error Analysis for the Physical Sciences*; McGraw-Hill: New York, 1969.
(39) Knyazev, V. D.; Bencsura, A.; Dubinsky, I. A.; Gutman, D.; Senkan, S. M. *Symp. Int. Combust. Proc.* **1994**, *25*, 817.
(40) Pople, J. A.; Scott, A. P.; Wong, M. W.; Radom, L. *Israel J. Chem.* **1993**, *33*, 345.
(41) Johnston, H. S. *Gas-Phase Reaction Rate Theory*; The Ronald Press: New York, 1966.
(42) Knyazev, V. D.; Bencsura, A.; Stoliarov, S. I.; Slagle, I. R. *J. Phys. Chem.* **1996**, *100*, 11 346.
(43) Knyazev, V. D.; Slagle, I. R. *J. Phys. Chem.* **1996**, *100*, 16 899.
(44) Fukui, K. *Acc. Chem. Res.* **1981**, *14*, 363.
(45) Gonzalez, C.; Schlegel, H. B. *J. Phys. Chem.* **1990**, *94*, 5523.
(46) Eckart, C. *Phys. Rev.* **1930**, *35*, 1303.
(47) Foresman, J. B.; Frisch, A. E. *Exploring Chemistry With Electronic Structure Methods*, 2nd ed.; Gaussian, Inc.: Pittsburgh, PA, 1996.
(48) Marcus, R. A. *J. Chem. Phys.* **1968**, *72*, 891.
(49) Knyazev, V. D.; Bencsura, A.; Slagle, I. R. *J. Phys. Chem. A* **1997**, *102*, 1760.
(50) *Thermodynamic Properties of Individual Substances;* Gurvich, L. V., Veyts, I. V., Alcock, C. B. Ed.; Eds.; Hemisphere: New York, 1992; Vol. Part 2.
(51) Chase, M. W., Jr. *J. Phys. Chem. Ref. Data* **1998**, *Monograph 9*, 1.
(52) Chettur, G.; Snelson, A. *J. Phys. Chem.* **1987**, *91*, 3483.
(53) Quelch, G. E.; Gallo, M. M.; Schaefer, H. F., III *J. Am. Chem. Soc.* **1992**, *114*, 8239.
(54) Knyazev. V. D.; Slagle, I. R. *J. Phys. Chem. A* **2001**, *105*, 6490.